https://doi.org/10.1016/j.ijthermalsci.2015.08.001

Exploration on the Reverse Calculation Method of Groundwater Velocity By Means of the Moving Line Heat Source

Wenke Zhang[a, *], Hongxing Yang[a], Nairen Diao[b], Lin Lu[a] and Zhaohong Fang[b]

a. Renewable Energy Research Group, The Hong Kong Polytechnic University, Hong Kong, China
b. Key Laboratory of Renewable Energy Utilization Technologies in Buildings, Ministry of Education, Shandong Jianzhu University, Jinan, China

Phone: 00852 2766 4698. Fax: 00852 2774 6146
Email: wenkezhang2006@163.com
* Corresponding author

Abstract The research on the influence that groundwater exerts on borehole ground heat exchanger has been made progress. However, the investigation on how to obtain the groundwater velocity is a little. According to the line heat source model with groundwater flow, a new methodology is explored to obtain the value and direction of groundwater velocity while it flows through borehole. Some points are distributed around borehole and they have the same distance to the center line of borehole, and the temperature responses of these points are significant parameters which lay firm foundation for reverse-reasoning. The reverse-reasoning calculation can be conducted by establishing objective function. The comparisons of temperature responses between theoretical results and the simulative recorded data are made. The impact degree of groundwater flow can be displayed and then the velocity is estimated. Differences among points' temperature responses are made full use of to respectively indicate the direction and value ranges of velocity. The relativity between the points' location and the velocity intensity is investigated and then some cases are chosen as the trials to verify the rationality of reverse calculation method. To a large extent, the research work of this paper provides theoretical guidance or computing mode for getting velocity of groundwater. The methodology can be employed for obtaining the velocity in actual engineering projects or other cases.

Keywords: ground heat exchanger**,** groundwater, reverse calculation, objective function, squared deviation, line source.

Nomenclature

x, y, z	rectangular coordinate (m)
X, Y, Z	dimensionless rectangular coordinate
q_l	heating rate per meter line heat source (W m^{-1})
k	thermal conductivity (W m^{-1} K^{-1})
r	distance between point and borehole center (m)
a	thermal diffusivity (m^2 s^{-1})
c_p	specific heat (J kg^{-1} K^{-1})
Fo	Fourier number
t_0	initial temperature (K)
t	temperature (K)
u	value of groundwater velocity (m/s)
U	dimensionless value of groundwater velocity
P	Green function with groundwater convection
S	sum of squared deviation
L	dimensionless distance

Greek symbols

τ	time (s)
φ	angle of groundwater velocity
Θ	dimensionless excess temperature
θ	excess temperature (K)

Superscript

$'$	integration parameter

Subscripts

i	infinite line source seepage model
rec	obtain based on simulative recorded data
cal	obtain based on calculation model
$1,2,3$	order number of points

1. Introduction

The ground source heat pump (GSHP) system avails itself of underground medium to achieve thermal discharge and heat absorption respectively in summer and in winter, and underground heat exchange occurs between ground heat exchangers (GHEs) and the surrounding medium. It is commonly believed that GHEs are significant components of the whole system, and their heat transfer performance greatly determines the behavior of GSHP technology. Currently the relevant models of GHEs are based on pure conduction; a large number of scholars and engineering technologists have realized that groundwater seepage exerts a considerable degree impact on thermal transmission performance of GHEs, and these researchers suggested a given mass of qualitative analysis. However, a little investigation on this problem has been done due to the calculation complexity. In addition, it is difficult to comprehend the local groundwater velocity and therefore the seepage intensity cannot be obtained even if mathematical models are employed. Borehole GHEs with the depth range from 60 m to 200 m are widely adopted in the GSHP engineering projects [1] and the groundwater seepage phenomenon exists more or less in such a deep strata, especially in coastal areas or groundwater rich areas where the groundwater can flow through underground medium. The heat transfer performance of GHEs can be improved by groundwater seepage due to convection; the stronger the seepage, the better the improvement degree to heat transfer process. In particular, the unbalance of endothermic and exothermic accumulation of GHEs can be alleviated so that the design size of GHEs is reduced.

At present, the research on calculation models of borehole GHEs with groundwater flow has been made progress. Firstly, the energy equations including the Green function were applied to obtain the transient temperature response caused by the line source [2,3]. Secondly, the heat transfer period of borehole GHEs is regarded as a complicated and unsteady process. Thirdly, conduction and convection synthetically constitute the heat exchange style during the time scale which is usually from months to years [4]. There is no doubt that groundwater seepage alleviates heat accumulation around GHEs. Accordingly, heat transfer performance can be improved. As for groundwater, it can ensure the sustainability of borehole GHEs even the velocity is low[5]; it can exert influence on the heat transfer of energy pile and improve the corresponding performance either [6]; the coupled conduction and groundwater advection from GHE to the surrounding soil have been studied, and the heat transfer performance is better than that of only pure conduction[7]. However, the test for groundwater velocity is difficult because the velocity always has minor order of magnitude and the underground structure is complicated; the specific value and orientation of velocity are hardly obtained. Thus, some calculations or analyses with the help of mathematical models cannot provide convincing basis, which means that how favorable to heat transfer performance is the groundwater flow cannot be shown. Accordingly, it is necessary to explore how to obtain relatively accurate groundwater velocity.

According to the existing models, a new reverse calculation method is proposed to estimate the value and orientation of groundwater velocity. Groundwater flows through borehole GHE and convection action has non-ignorable influence on the distribution of temperature field [8]. If the temperature responses of some points locating near the borehole GHE can be recorded, the comparisons between recorded data and the temperature response obtained by mathematical models can be made, the recorded data are those measured values. The objective function is established and it aims at comparing the difference between recorded data and theoretical data. Although the accurate velocity is unknown at first, as the iteration proceeds, that is, velocity can be selected continually from the pre-set range sufficiently covering all the possible velocities, the accurate velocity can be determined while the difference reaches the minimal value. Thereby, this is a novel reverse calculation method to acquire groundwater velocity. The experimental data need to be recorded are temperatures of some points which are close to borehole, the thermal resistors can be installed at these points and the data collecting instrument is employed to obtain the corresponding data. The fluid inside U-tube of borehole circulates to emit heat and therefore the temperature response outside borehole can be achieved, but it is not necessary to take fluid temperature into account.

The application significance of the reverse calculation method is to obtain the groundwater velocity by way of testing some points' temperatures, and then the heat transfer performance of borehole GHE can be analyzed while groundwater flows through it.

The study combined with computer programming is conducted in the process of exploration. It is conceivable that the concrete values and orientation of groundwater velocity are respectively achieved. Once the problem of getting velocity is solved, the improvement degree caused by groundwater flow to heat transfer performance of borehole GHEs can be vividly expressed. As a result, the design size of borehole GHEs is reduced so that the initial cost of the whole GSHP system is reduced [9]. From what has been analyzed above, it is necessary to explore the reverse calculation method to obtain the velocity.

2. Interpretation of methodology

2.1. The schematic diagram of distributing points

Underground hydraulic gradient leads to groundwater seepage [10]. The greater the gradient, the larger the velocity value, and the orientation of seepage rests with gradient direction. Groundwater flows along three-dimensional directions or even in rough-and-tumble manner sometimes, but basically the gradient direction is at one plane and therefore the two-dimensional seepage should be taken into account. Three points with the same radius r to the center of borehole are set around borehole GHE to fulfill the reverse-reasoning, and the 120-degree intersection angle between every two neighboring points is defined. It is clear that the effect is better if added points with well-distributed intersection angle are arranged around borehole, because this can ameliorate reverse-reasoning result. However, the arrangement difficulty is increased in case a number of points are selected near borehole underground, and the temperature response difference between neighboring points is tiny when groundwater flows through borehole. Accordingly, it is suggested that three points are chosen to test and verify the reverse calculation effect, and the diagram is shown in Fig.1.

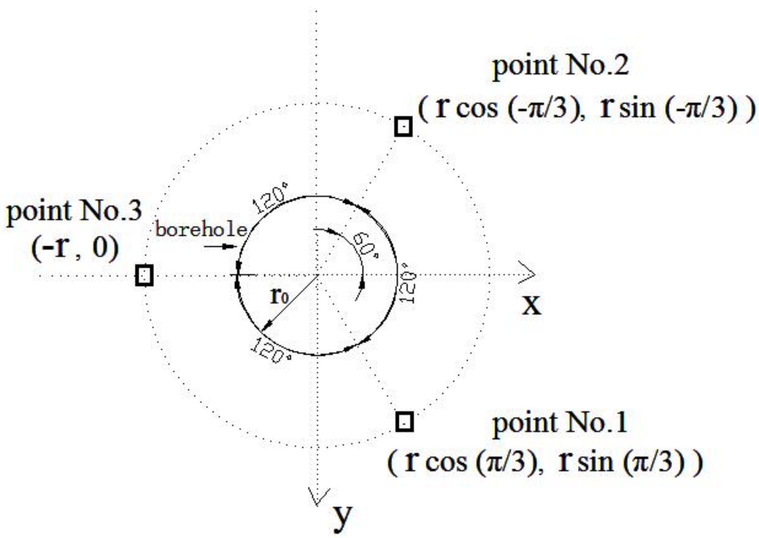

Fig.1 The schematic diagram on distributing points

2.2. The applicable calculation models

The mode mentioned in Fig.1 is the necessary precondition of conducting reverse-reasoning. Then, the theoretical calculation models should be reported. Borehole GHE are usually deemed as the line heat sources and therefore the moving line source model is taken into consideration while groundwater flows through borehole [11]. If one point source with the coordinate (x', y', z') emits heat from the time τ', when groundwater presents the intersection angle φ with the positive direction of x-axis, the temperature response at any point (x, y, z) except heat source can be displayed by the form of Green function in the event of groundwater flow, i.e. Eq.(1):

$$P(x,y,z,\tau;x',y',z',\tau')=\frac{1}{8[\pi a(\tau-\tau')]^{3/2}}\cdot\exp\left\{-\frac{[x-x'-u\cos\varphi(\tau-\tau')]^2+[y-y'-u\sin\varphi(\tau-\tau')]^2+(z-z')^2}{4a(\tau-\tau')}\right\} \tag{1}$$

Accordingly, the analytical solution of the infinite moving line source model is listed in Eq.(2) and q_l denotes the heat transfer quantity per meter borehole GHE.

$$\theta_i=\frac{q_l}{\rho c}\int_0^{\tau}d\tau'\int_{-\infty}^{\infty}\frac{1}{8\left[\pi a(\tau-\tau')\right]^{3/2}}\cdot\exp\left[-\frac{[x-x'-u\cos\varphi(\tau-\tau')]^2+[y-y'-u\sin\varphi(\tau-\tau')]^2+(z-z')^2}{4a(\tau-\tau')}\right]dz' \tag{2}$$

where $\theta_i = t - t_0$, t and t_0 are transient temperature and initial temperature, respectively.

The line source locates at z-axis and thus the Eq.(2) can be changed into Eq.(3).

$$\theta_i=\frac{q_l}{4\pi k}\int_0^{\tau}\frac{1}{(\tau-\tau')}\exp\left[-\frac{[x-u\cos\varphi(\tau-\tau')]^2+[y-u\sin\varphi(\tau-\tau')]^2}{4a(\tau-\tau')}\right]d\tau' \tag{3}$$

The expression of Eq.(3) in cylindrical coordinate is shown in Eq.(4).

$$\theta_i=\frac{1}{4\pi}\int_0^{\tau}\frac{1}{(\tau-\tau')}\exp\left[-\frac{[r\cos\beta-u\cos\varphi(\tau-\tau')]^2+[r\sin\beta-u\sin\varphi(\tau-\tau')]^2}{4a(\tau-\tau')}\right]d\tau' \tag{4}$$

where β is the angle from the positive direction to the point location, r is the radius between point location and borehole center.

To reduce the number of parameters and simplify the expression, non-dimensional parameters are introduced such as: $\Theta_i = k\,\theta_i / q_l$, $U = u\,r / a$, $Fo = a\tau / r^2$. The dimensionless formula is shown in Eq.(5).

$$\Theta_i=\frac{1}{4\pi}\int_0^{Fo}\frac{1}{(Fo-Fo')}\exp\left[-\frac{\left[\cos\theta-U\cos\varphi(Fo-Fo')\right]^2+\left[\sin\theta-U\sin\varphi(Fo-Fo')\right]^2}{4(Fo-Fo')}\right]dFo' \tag{5}$$

2.3 The objective function and reverse-reasoning procedure

The temperature response data of these points with the time can be recorded if three points have been distributed. The range needs to be respectively set for value and orientation as the specific velocity is unknown. For example, the range is usually from 10^{-6} m /s to 10^{-2}m /s on the basis of local geological information, therefore this range can be set in advance for value-scale of velocity. The angle can be defined from -180° to 180° although the accurate angle is unknown, so clear it is that the intersection angle must be at this range. Because the test data are recorded at regular intervals, continuous iteration from the range of value and direction of groundwater velocity is done in the process of reverse-reasoning. Given that the difference between recorded data and calculation results achieves the minimum [12], the corresponding value and direction are respectively the actual data of groundwater. The expression of objective function is shownin Eq.(6)

$$S = \sum_{i=1}^{n} (\Theta_{cal,i} - \Theta_{rec,i})^2 \tag{6}$$

where $\Theta_{cal,\,i}$ and $\Theta_{rec,\,i}$ denote the non-dimensional temperatures of the model and the recorded data, respectively. Because $\Theta_{rec,\,i} = k\theta_i / q_1 = k(t - t_0) / q_1$, the non-dimensional value can be achieved if the transient temperature, initial temperature, thermal conductivity and heat transfer quantity per meter borehole GHE are obtained. Initial temperature can be taken note before running of GHEs, and transient temperature can be recorded at regular time intervals [13-15], obviously there are n values from No.1 to No.n. Thermal conductivity k is obtained by thermal test equipment and q_l can be calculated according to relevant parameters, the sample of underground medium can be put in the laboratory directly to observe and measure the corresponding thermophysical parameters by test instruments.

Three points are set around borehole and three objective functions are respectively established. If all the functions can achieve the minimum, then the corresponding value and direction are the actual cases. To be more specific, the values or directions meeting the minimum of only one point function may lead to many choices, that is, some different values and directions can let objective function of one point reach the minimum. Three objective functions are set and all of them arrive at the minimum; the acceptable velocity range for every point function maybe different with each other, but the intersection of three velocity ranges can produce the ultimate single velocity if only three ranges occur simultaneously. Eq.(2) is a binary function with two independent variables U and φ; S can make first order partial derivatives respectively towards parameter U and φ, and the corresponding signs can be indicated respectively by S^{U} and S^{φ} [16]. Thus, the necessary conditions for realizing the minimum of S are shown in Eq.(7).

$$\begin{cases} S^{U} = 0 \\ S^{\varphi} = 0 \end{cases} \tag{7}$$

It should be admitted that Eq.(7) is the necessary condition rather than the sufficient condition, and the velocities fulfilling Eq.(7) are named as stationary points. The stationary points which simultaneously satisfy the Eq.(7) of every different point maybe single or at a minor range. The detailed expressions of S^{U} and S^{φ} are respectively shown in Eq.(8) and Eq.(9).

$$\begin{aligned} S^{U} = {} & 2\sum_{i=1}^{n}(\Theta_{cal,i}-\Theta_{rec,i})\Theta_{cal,U}{}' = 2\sum_{i=1}^{n}\left(\frac{1}{4\pi}\int_{0}^{Fo_i}\frac{1}{(Fo_i-Fo')}\exp\left[\frac{\left[X-U\cos\varphi(Fo_i-Fo')\right]^2+\left[Y-U\sin\varphi(Fo_i-Fo')\right]^2}{4\left(Fo_i-Fo'\right)}\right]dFo'-\Theta_{rec,i}\right)\cdot \\ & \frac{1}{4\pi}\int_{0}^{Fo_i}\frac{1}{(Fo_i-Fo')}\exp\left[\frac{\left[X-U\cos\varphi(Fo_i-Fo')\right]^2+\left[Y-U\sin\varphi(Fo_i-Fo')\right]^2}{4\left(Fo_i-Fo'\right)}\right]\cdot \\ & \frac{2\cdot\left[X-U\cos\varphi(Fo_i-Fo')\right]\cdot\cos\varphi(Fo_i-Fo')+2\cdot\left[Y-U\sin\varphi(Fo_i-Fo')\right]\cdot\sin\varphi(Fo_i-Fo')}{4\left(Fo_i-Fo'\right)}dFo' \end{aligned} \tag{8}$$

$$\begin{aligned} S^{\varphi} = {} & 2\sum_{i=1}^{n}(\Theta_{cal,i}-\Theta_{rec,i})\Theta_{cal,i,\varphi}{}' = 2\sum_{i=1}^{n}\left\{\frac{1}{4\pi}\int_{0}^{Fo_i}\frac{1}{(Fo_i-Fo')}\exp\left[-\frac{\left[X-U\cos\varphi(Fo_i-Fo')\right]^2+\left[Y-U\sin\varphi(Fo_i-Fo')\right]^2}{4\left(Fo_i-Fo'\right)}\right]dFo'-\Theta_{rec,i}\right\}\cdot \\ & \frac{1}{4\pi}\int_{0}^{Fo_i}\frac{1}{(Fo_i-Fo')}\exp\left[-\frac{\left[X-U\cos\varphi(Fo_i-Fo')\right]^2+\left[Y-U\sin\varphi(Fo_i-Fo')\right]^2}{4\left(Fo_i-Fo'\right)}\right]\cdot \\ & \frac{-2\cdot\left[X-U\cos\varphi(Fo_i-Fo')\right]\cdot U\sin\varphi(Fo_i-Fo')+2\cdot\left[Y-U\sin\varphi(Fo_i-Fo')\right]\cdot U\cos\varphi(Fo_i-Fo')}{4\left(Fo_i-Fo'\right)}dFo' \end{aligned} \tag{9}$$

In addition to objective function mentioned in Eq.(6), another way is to set the total sum of squared deviations of three points, i.e. Eq.(10).

$$S=\sum_{i=1}^{n}(\Theta_{cal,i,1}-\Theta_{rec,i,1})^2+(\Theta_{cal,i,2}-\Theta_{rec,i,2})^2+(\Theta_{cal,i,3}-\Theta_{rec,i,3})^2 \tag{10}$$

However, there is just one function shown in Eq.(10), thus the possibility of producing an error may be higher than that of respectively establishing object function of every point. The velocity obtained by function of every point can be verified with each other if functions are respectively set up, therefore the intersection is more accurate than the result of only function and it is suggested that three functions are respectively established.

In theory, the actual velocity can be achieved by reverse-reasoning according to the first order partial derivatives, but the values and directions of velocities which conform to Eq.(7) may not be single. Maybe some cases can be found and then the single concrete actual case cannot be confirmed. For this reason, the second order partial derivatives are employed; firstly, S^{UU} means the second order partial derivative towards U; secondly, $S^{U\varphi}$ is the second order partial derivative towards U and φ mixed; thirdly, $S^{\varphi\varphi}$ delegates the second order partial derivative towards φ. The detailed expansion equations are respectively shown in Eq.(11), Eq.(12) and Eq.(13).

$$
S^{UU} = 2\sum_{i=1}^{n} \left\{ \begin{aligned}
&\left\{ \begin{aligned} &\frac{1}{4\pi}\int_0^{Fo_i} \frac{1}{(Fo_i - Fo')} \exp\left[-\frac{\left[X - U\cos\varphi(Fo_i - Fo')\right]^2 + \left[Y - U\sin\varphi(Fo_i - Fo')\right]^2}{4\left(Fo_i - Fo'\right)} \right] \cdot \\
&\frac{\left[X - U\cos\varphi(Fo_i - Fo')\right]\cdot\cos\varphi + \left[Y - U\sin\varphi(Fo_i - Fo')\right]\cdot\sin\varphi}{2} dFo' \end{aligned} \right\}^2 + \\
&\left\{ \frac{1}{4\pi}\int_0^{Fo_i} \frac{1}{(Fo_i - Fo')} \exp\left[-\frac{\left[X - U\cos\varphi(Fo_i - Fo')\right]^2 + \left[Y - U\sin\varphi(Fo_i - Fo')\right]^2}{4\left(Fo_i - Fo'\right)} \right] dFo' - \Theta_{rec,i} \right\} \cdot \\
&\left\{ \begin{aligned} &\frac{1}{4\pi}\int_0^{Fo_i} \frac{1}{(Fo_i - Fo')} \exp\left[-\frac{\left[X - U\cos\varphi(Fo_i - Fo')\right]^2 + \left[Y - U\sin\varphi(Fo_i - Fo')\right]^2}{4\left(Fo_i - Fo'\right)} \right] \cdot \\
&\left[\frac{\left[X - U\cos\varphi(Fo_i - Fo')\right]\cdot\cos\varphi + \left[Y - U\sin\varphi(Fo_i - Fo')\right]\cdot\sin\varphi}{2} \right]^2 dFo' \\
&+ \frac{1}{4\pi}\int_0^{Fo_i} \frac{1}{(Fo_i - Fo')} \exp\left[-\frac{\left[X - U\cos\varphi(Fo_i - Fo')\right]^2 + \left[Y - U\sin\varphi(Fo_i - Fo')\right]^2}{4\left(Fo_i - Fo'\right)} \right] \cdot \\
&\frac{-(Fo_i - Fo')}{2} \end{aligned} \right\}
\end{aligned} \right\} \quad (11)
$$

$$
\begin{aligned}
S^{U\varphi} = 2\sum_{i=1}^{n} \Bigg\{ & \left\{ \frac{1}{4\pi}\int_0^{Fo_i}\frac{1}{(Fo_i-Fo')}\exp\left[-\frac{\left[X-U\cos\varphi(Fo_i-Fo')\right]^2+\left[Y-U\sin\varphi(Fo_i-Fo')\right]^2}{4\left(Fo_i-Fo'\right)}\right]\cdot\frac{YU\cos\varphi-XU\sin\varphi}{2}dFo' \right\}\cdot \\
& \frac{1}{4\pi}\int_0^{Fo_i}\frac{1}{(Fo_i-Fo')}\exp\left[-\frac{\left[X-U\cos\varphi(Fo_i-Fo')\right]^2+\left[Y-U\sin\varphi(Fo_i-Fo')\right]^2}{4\left(Fo_i-Fo'\right)}\right]\cdot\frac{X\cos\varphi-U(Fo-Fo')+Y\sin\varphi}{2}dFo' \\
& +\left\{ \frac{1}{4\pi}\int_0^{Fo_i}\frac{1}{(Fo_i-Fo')}\exp\left[-\frac{\left[X-U\cos\varphi(Fo_i-Fo')\right]^2+\left[Y-U\sin\varphi(Fo_i-Fo')\right]^2}{4\left(Fo_i-Fo'\right)}\right]dFo'-\Theta_{rec,i} \right\}\cdot \\
& \Bigg\{ \frac{1}{4\pi}\int_0^{Fo_i}\frac{1}{(Fo_i-Fo')}\exp\left[-\frac{\left[X-U\cos\varphi(Fo_i-Fo')\right]^2+\left[Y-U\sin\varphi(Fo_i-Fo')\right]^2}{4\left(Fo_i-Fo'\right)}\right]\cdot\frac{YU\cos\varphi-XU\sin\varphi}{2}\cdot \\
& \frac{X\cos\varphi-U(Fo_i-Fo')+Y\sin\varphi}{2}dFo'+ \\
& \frac{1}{4\pi}\int_0^{Fo_i}\frac{1}{(Fo_i-Fo')}\exp\left[-\frac{\left[X-U\cos\varphi(Fo_i-Fo')\right]^2+\left[Y-U\sin\varphi(Fo_i-Fo')\right]^2}{4\left(Fo_i-Fo'\right)}\right]\cdot\frac{Y\cos\varphi-X\sin\varphi}{2} \Bigg\} \Bigg\}
\end{aligned}
\tag{12}
$$

$$
\begin{aligned}
S^{\varphi\varphi} = 2\sum_{i=1}^{n} \Bigg\{ & \left\{ \frac{1}{4\pi}\int_0^{Fo_i}\frac{1}{(Fo_i-Fo')}\exp\left[-\frac{\left[X-U\cos\varphi(Fo_i-Fo')\right]^2+\left[Y-U\sin\varphi(Fo_i-Fo')\right]^2}{4\left(Fo_i-Fo'\right)}\right]\cdot\frac{YU\cos\varphi-XU\sin\varphi}{2}dFo' \right\}^2 \\
& +\left\{ \frac{1}{4\pi}\int_0^{Fo_i}\frac{1}{(Fo_i-Fo')}\exp\left[-\frac{\left[X-U\cos\varphi(Fo_i-Fo')\right]^2+\left[Y-U\sin\varphi(Fo_i-Fo')\right]^2}{4\left(Fo_i-Fo'\right)}\right]dFo'-\Theta_{rec,i} \right\}\cdot \\
& \Bigg\{ \frac{1}{4\pi}\int_0^{Fo_i}\frac{1}{(Fo_i-Fo')}\exp\left[-\frac{\left[X-U\cos\varphi(Fo_i-Fo')\right]^2+\left[Y-U\sin\varphi(Fo_i-Fo')\right]^2}{4\left(Fo_i-Fo'\right)}\right]\cdot\left[\frac{YU\cos\varphi-XU\sin\varphi}{2}\right]^2dFo' \\
& +\frac{1}{4\pi}\int_0^{Fo_i}\frac{1}{(Fo_i-Fo')}\exp\left[-\frac{\left[X-U\cos\varphi(Fo_i-Fo')\right]^2+\left[Y-U\sin\varphi(Fo_i-Fo')\right]^2}{4\left(Fo_i-Fo'\right)}\cdot\frac{-YU\sin\varphi-XU\cos\varphi}{2}\right]dFo' \Bigg\} \Bigg\}
\end{aligned}
\tag{13}
$$

This is a method of finding extreme values and it is equal to recognized steepest descent method. The single velocity may be found after adopting the first order partial derivative. It is not necessary to employ the second order partial derivative if this case appears. However, some velocities adapt themselves to the conditions of the first order partial derivative, that is, several different velocities or a range of velocities appear and therefore the single velocity cannot be confirmed. Afterwards, these stationary points should be brought into the formulas of the second order partial derivative, such as: S^{UU} (stationary points) = A, $S^{U\varphi}$ (stationary points) = B and $S^{\varphi\varphi}$ (stationary points) = C. The extremum of Eq.(6) appears in case A*C-B^2 > 0. On the one hand, the minimum of Eq.(6) can be achieved if A > 0 is true; on the other hand, the maximum exists when A < 0 [17]. In general, it is easy to further limit the velocities if the second order partial derivatives of three points are utilized simultaneously. Therefore, the groundwater velocity can be determined according to both the first and the second order partial derivatives.

One fact is that the two parameters U and φ are respectively discrete variables rather than continuous variables; it is difficult to let the both S^U and S^φ achieve the zero absolutely. However, these two values can reach a very minor value maybe nearly zero, therefore a minor value such as 0.01 or 0.005 and so on can be set for S^U and S^φ; this minor value can be constantly reduced to further narrow the range of U and φ. The values for U and φ maybe confirmed or limited to a minor rang in such a way, and then the second order partial derivatives of three points are all employed to find the actual U and φ. Admittedly, the worst case is that the single U and φ cannot be determined after utilizing both the first and the second order partial derivatives, which means there still exists a minor range. The only method is that the remaining numerical values of the range are put into Eq.(6) of three points if this case occurs, the corresponding results can be acquired by using these values one by one. These calculation results are compared with each other to find the minimum and then the corresponding U and φ are the final findings. The underground thermal conductivity can be obtained by thermal physical tester which is an instrument that has been widely employed in the engineering projects.

3. The analysis on relevant characteristics

3.1 The relativity between points radius and velocity intensity

The distance from the points to the borehole center is worthy discussing because this problem has an influence on the test and calculation result. It is possible to explore the relationship between this distance and velocity intensity by way of relevant equations. Because the angle of groundwater seepage is from -180˚ to 180˚, in the process of analyzing the relativity some angles can be selected for discussing. The analysis is based on 15˚ interval within the angle range and then some angles such as -180˚, -165˚ and so on are employed. It is advisable that the dimensionless value of velocity should be from 0.1 to 3.0 through investigation. The velocity can attain the value of 10 while it is too large, and it is nearly equal to 0 if the groundwater seepage is too weak [18]. Accordingly, the range from 0.1 to 3.0 meets the reasonable range of dimensionless groundwater velocity. Because U is equal to ur / a, the product of actual velocity value and point radius should be at the range from

0.1a to 3a. On the one hand, the temperature response difference of three points is minor even little if the value of U is less than 0.1, which is unfavorable for conducting reverse-reasoning. On the other hand, the temperature response is weak due to the groundwater convection when U is greater than 3.0. The range from 0.1 to 3.0 is proven to be suitable for all the angles of groundwater seepage. To exhibit the temperature response of three points, two extreme values of U , that is, 0.1 and 3.0, are chosen to illustrate the relevant circumstances shown in Fig.2. Because the angles with 15° interval between -180° and 180°are all tested and every angle has the corresponding range of velocity, the range from 0.1 to 3.0 is the intersection of all ranges and therefore 0° orientation of groundwater velocity is employed to display the temperature responses of three points.

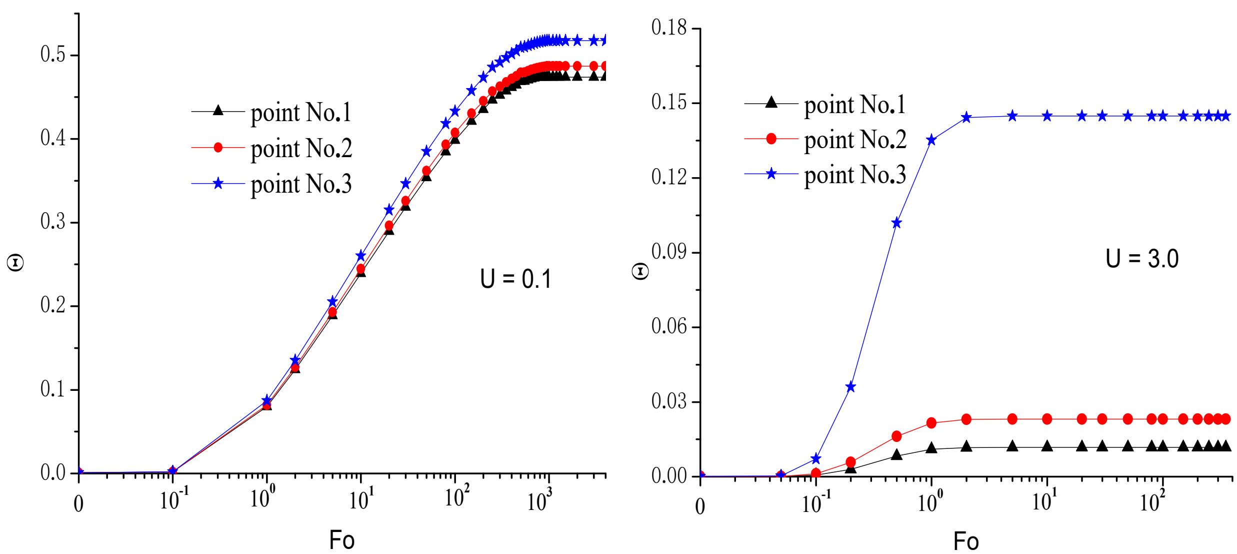

Fig.2 The temperature responses of three points when U adopts two extreme values

There is a belief that other circumstances are between these two cases, the relativity between points' radius and velocity intensity can be summarized, that is, their product should be in the range between 0.1a and 3.0a.

3.2 The research on flex points of the temperature response curves

According to the temperature response curves given in Fig.2, the temperature responses of points firstly go through the process of increasing slope and then they keep the slope decreased continuously, at last all temperature responses attain the stable states, which means the last status is steady. It is significant to find the flex points because the temperature response degree at different stage can be understood [19]. From the perspective of mathematics, the so-called flex points are those points at which the concave-convex deformation occurs in function curves. If one function has both the first order and the second order derivative in a certain coordinate interval for independent variable, the function curve presents concave while the second order derivative keep positive value, or else the negative value of the second order derivative lead to the convex trend of function curve. Therefore, the location which makes the second order derivative be equal to zero is titled flex point. The Eq.(5) is taken into account for investigating the relationship between the flex point and the time, the parameter *F*o is independent variable and Θ_i delegates the function value. The first order derivative towards *F*o is firstly conducted and the corresponding formula is shown in Eq.(14)

$$\Theta_{cal,i}{}^{Fo} = \frac{1}{4\pi} * \frac{1}{Fo} * \exp\left[-\frac{\left(\cos\theta - U * \cos\varphi * Fo\right)^2 + \left(\sin\theta - U * \sin\varphi * Fo\right)^2}{4Fo} \right] \tag{14}$$

After that, the second order derivative is obtained in Eq.(15) based on Eq.(14).

$$\begin{aligned} \Theta_{cal,i}{}^{FoFo} = & -\frac{1}{4\pi} \cdot \frac{1}{Fo^2} \cdot \exp\left[-\frac{\left(\cos\theta - U \cdot \cos\varphi \cdot Fo\right)^2 + \left(\sin\theta - U \cdot \sin\varphi \cdot Fo\right)^2}{4Fo} \right] + \frac{1}{16\pi} \cdot \frac{1}{Fo} \cdot \exp\left[-\frac{\left[\cos\theta - U \cdot \cos\varphi \cdot Fo\right]^2 + \left[\sin\theta - U \cdot \sin\varphi \cdot Fo\right]^2}{4Fo} \right] \cdot \\ & \left[\frac{2U \cdot \cos\varphi \cdot Fo \cdot \left(\cos\theta - U \cdot \cos\varphi \cdot Fo\right) + \left(\cos\theta - U \cdot \cos\varphi \cdot Fo\right)^2}{Fo^2} + \frac{2U \cdot \sin\varphi \cdot Fo \cdot \left(\sin\theta - U \cdot \sin\varphi \cdot Fo\right) + \left(\sin\theta - U \cdot \sin\varphi \cdot Fo\right)^2}{Fo^2} \right] \end{aligned} \tag{15}$$

Sometimes *F*o cannot fulfill the zero value of the second order derivative, in this case the method of bisection is employed in the positive and negative boundaries of the second order derivative, consequently the approximate *F*o can be acquired. The explorations on the relationship between flex point and the time for three points are all conducted. It can be summarized that the flex point location is only related with the velocity value *U* of groundwater and is hardly affected by groundwater seepage angle *φ*. This conclusion is the same no matter which point around borehole is used for calculating and analyzing. The relevant curve demonstrating the process which *F*o changes with *U* is shown in Fig.3. To conveniently and clearly unfold the correlation between *U* and *F*o, the horizontal coordinate takes Lg(*U*) as the objective while *F*o is regarded as the value of longitudinal coordinate. The phenomenon is *F*o of flex point remains nearly the same while the velocity intensity is not large enough, but *F*o of flex point drops rapidly if *U* achieves a certain order of magnitude.

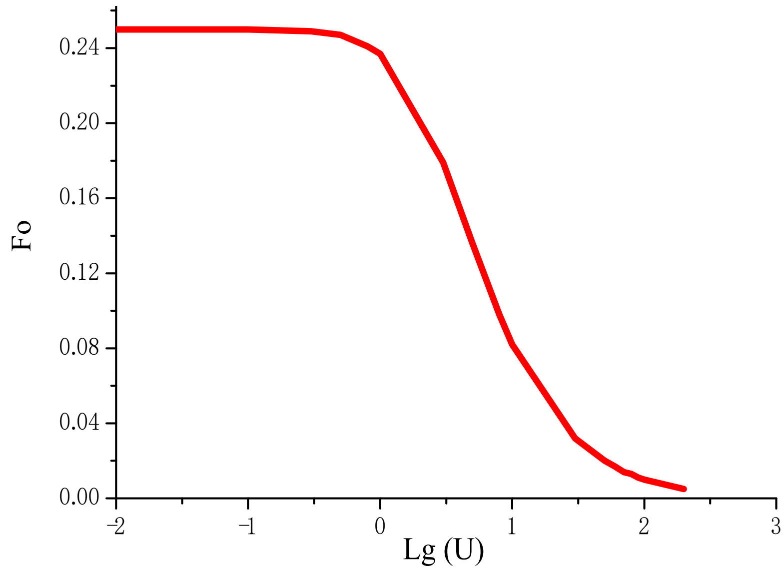

Fig.3 The variation trend which *F*o changes with Lg (*U)*

Another significant coordinate concerning the correlation between velocity value *U* and the product of flex point's *U* and *Fo* can be established, and the detailed information is shown in Fig.4. Lg(*U*) is still employed as the horizontal coordinate meanwhile product of *U* and *Fo* is used as longitudinal coordinate. It is reported in Fig.4 that *L* increases with *U* until arrive at stable state, it firstly experienced the process that slope keeps increasing and then went into the decreasing slope stage. From this phenomenon, the *F*o of the flex point is inversely proportional to *U* while the groundwater seepage velocity attains enough intensity.

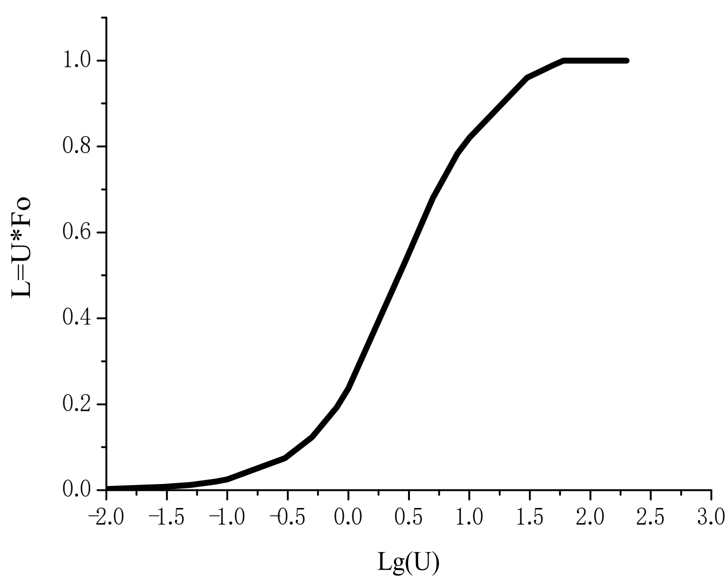

Fig.4 The variation of the product of *U* and *F*o with Lg (*U*)

3.3 The relationship between the time of reaching half of stable temperature response and the velocity intensity

The groundwater seepage has a convection impact on thermal exchange process and the temperature response will arrive at steady state eventually [20]. Both the stable response value and the time needed for achieving a steady state depend on the velocity intensity. The temperature response increases promptly in the early period according to the response curves above, thereby the response data of this stage is more effectual than those of late period to conduct reverse-reasoning. The response curves keep the slope increasing and thus the differences of these data calculated or recorded at set internal are evident. The clearer the data difference at different moment, the better the reverse-reasoning result. On the whole, the half value of temperature response can be selected to observe the corresponding time. Because the whole response curves experience the stage with increasing slope and then goes through the decreasing slope period, the time needed for attaining half of stable temperature response is far less than that of achieving another half temperature rise. From another view, the data recorded from the initial moment to the time of attaining the first half temperature rise is more valuable to realize reverse-reasoning. Therefore, it is necessary to observe the relations between the time of the half of stable temperature response and the velocity intensity, and the corresponding curve is shown in Fig.5.

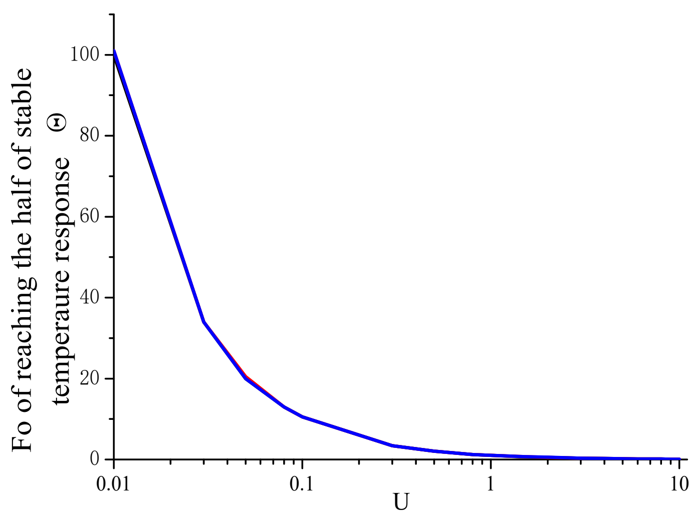

Fig.5 *F*o of reaching the half of stable temperature response changes with *U*

The relevant calculation and exploration on three points were conducted while different seepage angles were assigned to groundwater, it should be noted that the variation trend is only related with the velocity intensity and is hardly affected by seepage angle or point location.

4. Preliminary judgment on orientation and value of groundwater velocity

4.1 The determination on range of angle of groundwater seepage

The orientation of groundwater seepage is also from -180˚ to 180˚ and the seepage angle has an important influence on temperature field around borehole GHE [21,22]. The following figures give a brief image on the temperature field's difference that orientation induced. There are three examples for the orientation such as 0˚, 45˚ and 90˚. The diagrams and the corresponding temperature distributions are revealed in Fig.6 and Fig.7, respectively. The temperatures of three points change with the orientation of groundwater.

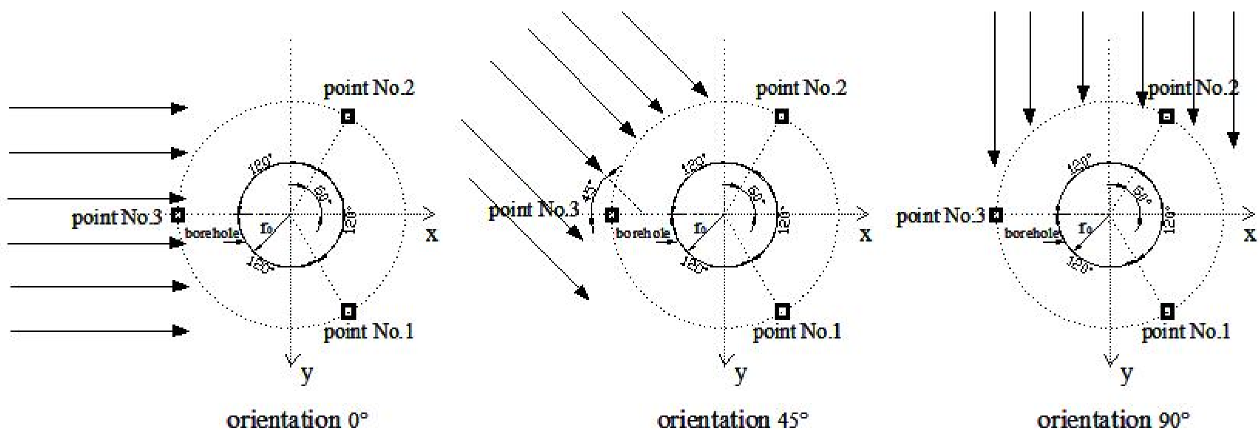

Fig.6 The diagram of different groundwater orientations

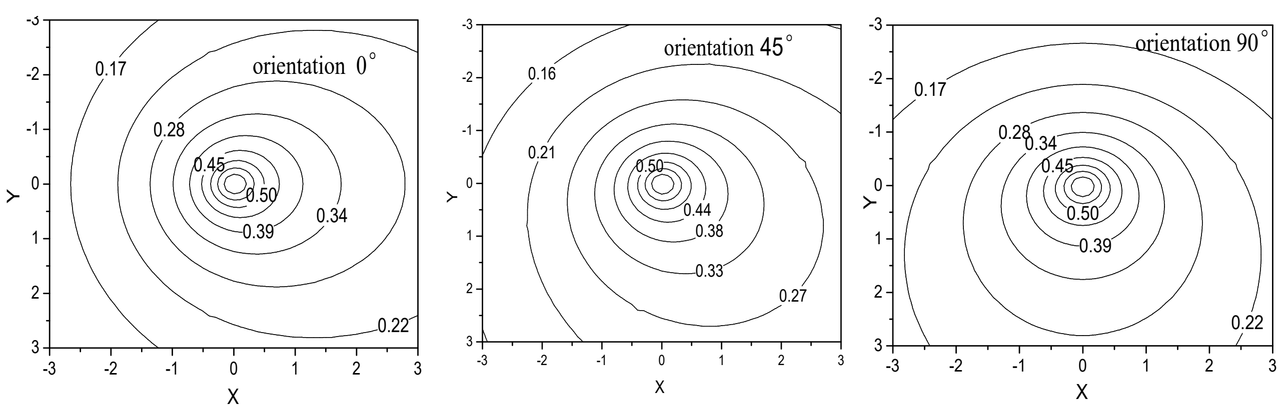

Fig.7 The temperature field while groundwater orientation adopts different angles

Though the accurate direction cannot be obtained at that time, it is necessary to make a brief judgment on the orientation range before making a reverse-reasoning calculation. Considering that there are totally three points distributed around borehole, the temperature response differences of three points can be fully used to roughly estimate the orientation scope. Comparisons of three points' temperature responses always change with the groundwater orientation; the influence degree of groundwater convection on different points changes in case the groundwater orientation is adjusted. Fig.8 reveals the orientation range according to the temperature difference of every two points while velocity employs a certain value.

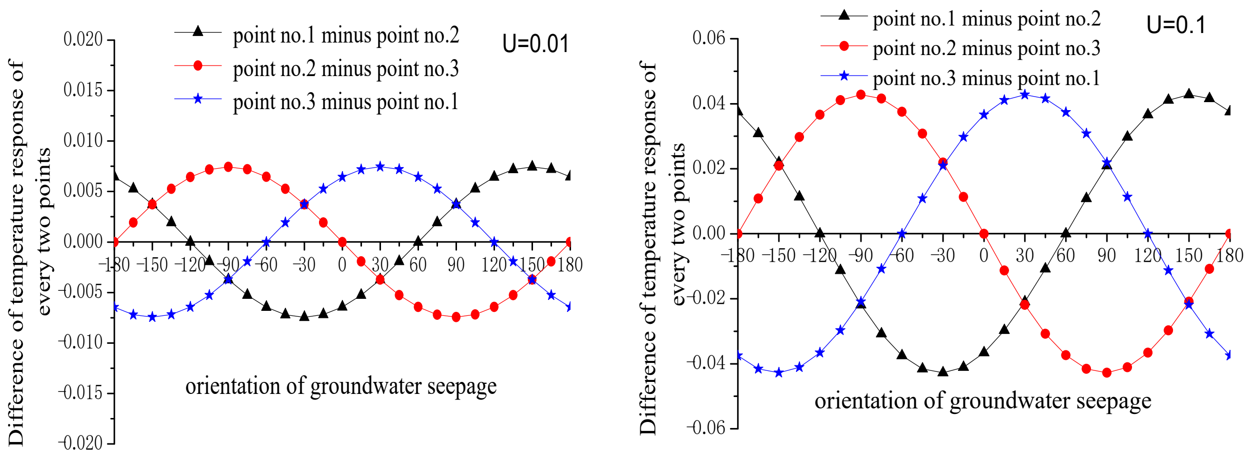

Fig.8 The influence of groundwater orientation on temperature differences of three points

Fig.8 shows that temperature responses' differences of three points are controlled to a certain extent by the orientation of groundwater flow, and the orientation effect becomes obvious gradually with the strengthening of velocity intensity. Accordingly, the preliminary orientation range of groundwater seepage can be judged and this can provide convenience for next reverse-reasoning.

4.2 The estimation on velocity intensity according to ratio of the maximal response to the minimal response

The value and orientation of groundwater velocity have effects on the temperature response of every point, that is, the response differences of points rest with the velocity. It is beyond question that the difference between the maximum response and the minimum response can show the intensity of seepage while orientation is constant [23, 24], thus the ratio of the maximum to the minimum is a significant parameter which can be adopted to estimate the velocity. The ratio increases with the velocity intensity U and the variation of seepage angles has little impact on the ratio. The relevant curves describing the relationship between the ratio and the velocity intensity are shown in Fig.9. Fig.9 shows that the ratio of the maximal temperature response to the minimal case change with the velocity. Θ_{max} and Θ_{min} are the maximal and the minimal dimensionless temperature responses, respectively, and U is the dimensionless velocity of groundwater.

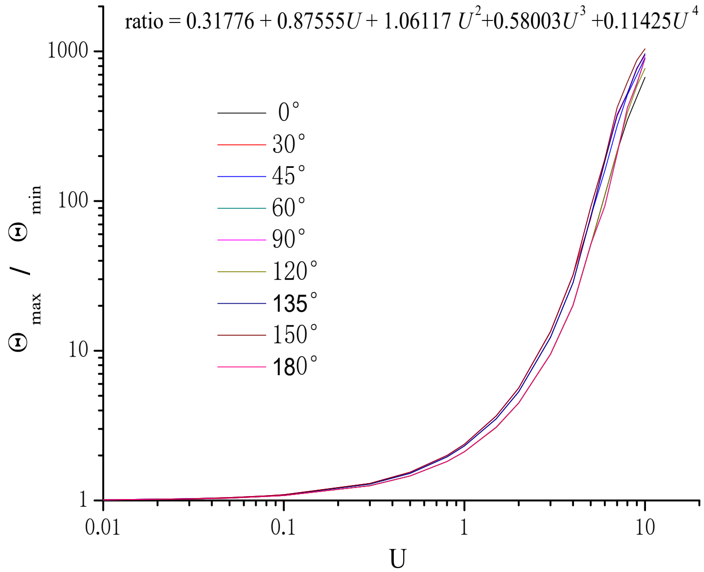

Fig.9 The variation trend of the ratios with *U*

Because the locations of three points are fixed and the orientation range of velocity is between -180˚ and 180˚, the orientation from -180˚ to 0˚ and from 0˚ and 180˚ are symmetrical in terms of exerting influence on temperature responses of three points. Different angles from the range between 0˚ and 180˚ can sufficiently prove the problem, that is, it is not necessary to select angles from -180˚ to 0˚ to analyze the orientation impact due to the symmetry, and some cases such as 0˚, 30˚, 45˚ and so on are chosen. At last, it can be certified that the difference of orientation has little influence on the ratio of the maximal response to the minimal response. A clear fitting formula is summarized to report the relationship between ratio and *U*, and it is given in Fig9 and Eq.(16) .

$$\text{ratio} = 0.31776+0.87555U+1.06117\,U^2+0.58003\,U^3+0.11425\,U^4 \tag{16}$$

5. The calculation trials

Some samples should be employed to validate the reverse calculation method, the temperature response of different times can be calculated according to Eq.(5) if the two important parameters U and φ of groundwater seepage are given. Firstly, U and φ can be respectively set as 0.1 and 45˚ at random, and then the response variation trend of three points with the time can be obtained. There is no actual experiment to record data at present but the simulative experimental data can be adopted, that is, the recorded data can be simulated by software though there is no actual data. It is universally acknowledged that there must be deviation or error between the theoretical data and the experimental recorded data, and the degree of deviation or error may be big or small. Commonly, the experimental recorded data fluctuates around theoretical data, accordingly the simulative recorded data can be achieved by simulation software though no actual experiment has been done until nowadays. Based on the curves obtained by means of the theoretical model i.e. Eq.(5), the random errors generated by software can be added on these theoretical values of three points and therefore the scatter diagram of simulative recorded data can be formatted, and the detailed information is shown in Fig.10.

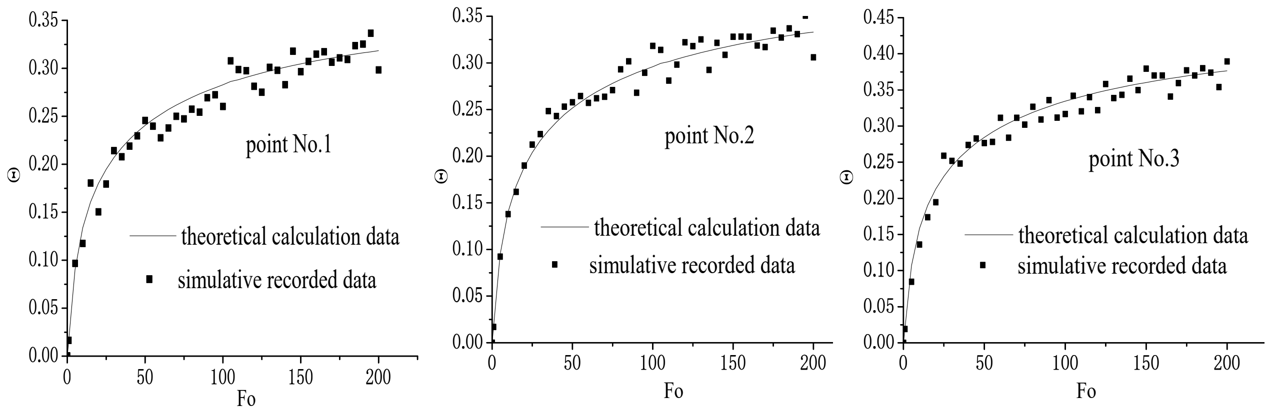

Fig.10 The temperature responses of both theoretical calculation and simulative recorded data (U=0.1, φ =45˚)

The theoretical curves are depicted based on the calculation results while different times are put into Eq.(5), and the simulative recorded data deviate from theoretical values and fluctuate to a certain extent. There are no actual experimental data but these simulative discrete scatters are similar to the experiment data [25-27]. Because the test time of these references is short and the data of only one point outside borehole is recorded, the references' data cannot be employed. Therefore, these scatters can be utilized as the simulative experimental data as the data can be recorded during the period of experiment while the time intervals are set. The random error with a relatively obvious degree is exerted on the theoretical value and thus there are a series of discrete variable that can be used to delegate the experimental recorded data. This is enough to simulate the actual experimental data. The accuracy of reverse calculation method can be more satisfied if the experiment time is long enough to record adequate data. By means of reverse-reasoning, the data that can let Eq.(6) achieve the minimum include U =0.1 and φ=42˚, 43˚,44˚, 45˚ and 46˚. The accurate value for the velocity intensity i.e. U can be obtained, but the exact orientation cannot be determined. However, the reverse-reasoning calculation have limited the orientation range to a very small scope; the median should be selected to diminish the estimation error of orientation of groundwater flow and thus 44˚ is derived. As a result, the effect of this example is satisfied though the last result is not entirely accurate; the value of groundwater velocity can be obtained correctly and the relative tolerance of groundwater orientation is only 2%.

Secondly, another example is still employed to further verify the methodology and this case is under the condition of U =1.0 and φ=30˚. The corresponding figures describing the temperature responses are shown in Fig.11.

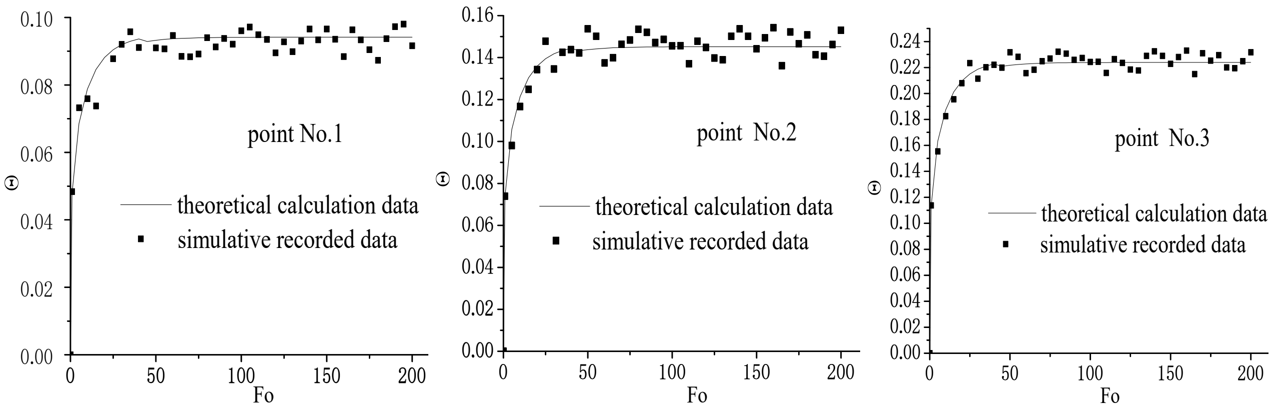

Fig.11 The temperature responses of both theoretical calculation and simulative recorded data (U=1.0, φ =30˚)

The degree of random error is larger than that of the first example and the results include several cases. There are five matches for U and φ, that is, (U=1.0, φ=30), (U=1.01, φ=29), (U=1.01, φ=30), (U=1.01, φ=31) and (U=1.02, φ=29). The match is not single but the range for U and φ are almost confined to a small scale, the medial values for U and φ are still preferred chosen. Thus, U=1.01 and φ=30 are the final results and the results of reverse calculation method are nearly equal to the actual cases. Therefore, the relative tolerance of groundwater value is only 1% and the groundwater orientation can be obtained correctly.

The last but not the least, the third example endows 0.5 and 60˚ respectively to U and φ, and the corresponding temperature responses are shown in Fig.12.

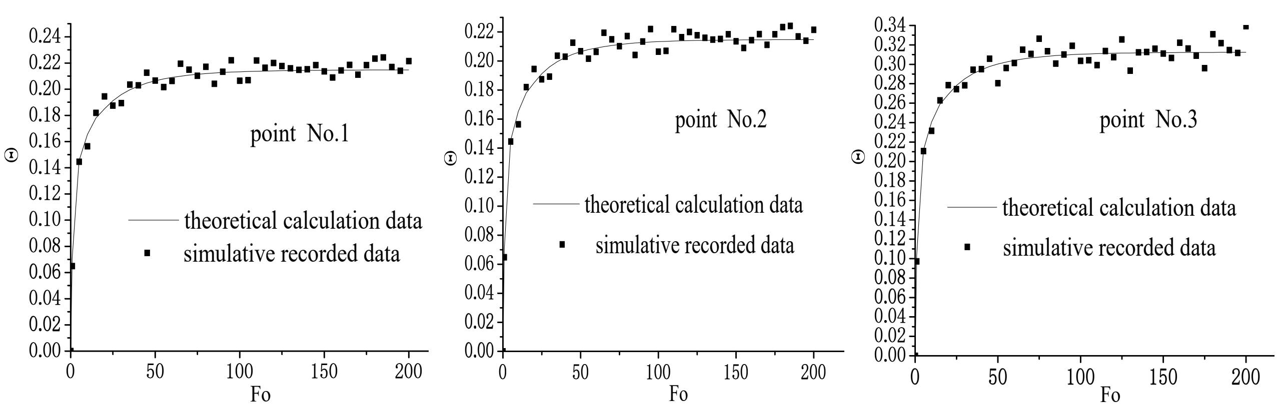

Fig.12 The temperature responses of both theoretical calculation and simulative experimental data (U=0.5, φ =60˚)

Fig.12 shows an obvious deviation between theoretical data and simulative recorded data, the ultimate finding after reverse-reasoning calculation indicates that the accurate values can be achieved, which means the calculation result is single, that is, U=0.5 and φ =60˚. Accordingly, the relative tolerance of this example is 0.

These examples prove that the reverse calculation method is reasonable. In the past, the inverse model of finite element method was employed to analyze the heat transfer problems; however, this inverse method uses adaptive meshing to conduct numerical simulation, and the values of a large number of meshes are iterated to find the final objects by means of inverse calculation [28]; this must increase the difficulty and therefore the time interval of process is long. Compared with this existing inverse model, the method introduced of this paper is more concise because only three points' temperature responses are needed, thus the time interval is shorter obviously. Accordingly, the methodology provides a sufficient theoretical basis for the prediction of groundwater velocity in any GSHP engineering project. Thermal resistors are installed at the points to record the temperatures. The PT 100 with the grade "A" or the PT 1000 can be used because their accuracies can attain around ±0.15℃ or better, that is to say, the accuracy of measurement can meet the requirement of conducting reverse-reasoning methodology. If the accuracy is less than this kind of accuracy of measurement, the effect of reverse calculation is affected.

6. Conclusions

The paper describes a detailed reverse calculation method for groundwater velocity. According to the moving line source model theory that describes the temperature response of borehole GHE under the condition of groundwater flow, the objective functions are established and then the method of getting extremum of multivariate function is employed, the first and the second order partial derivative are taken into consideration to lay a firm foundation for seeking the accurate velocity. Based on the temperature response curves of three points distributed around borehole GHE, the relevant characteristics involved in seepage phenomenon are analyzed and investigated. How to effectively employ three points is a noteworthy problem and therefore the influence that groundwater seepage exerts on every point can be explored in detail. The ranges of orientation and intensity of groundwater velocity can be preliminary confirmed to supply convenience for further discussion, and the serviceability of the reverse-reasoning can be verified to some extent. It should be admitted that added points well-distributed around borehole can produce better calculation result, but this will increase difficulty in setting points in actual engineering projects, in addition, this will lead to more complex procedure in terms of calculation. The trials are conducted to verify the methodology and three examples are employed while U and φ are endowed different values. It can be proven that the reverse calculation method is reasonable, and three points are enough to ensure the accuracy of methodology when the intersection angles between every two neighboring points are equal to each other and the random errors are adopted to simulate the experimental recorded data. The actual experiments have not been done for the moment and this is the next work for us. The content of this paper introduces a methodology and therefore provides a theory basis for next experiment or actual application in engineering projects. As long as the intensity U and orientation φ of groundwater velocity are calculated by reverse calculation method, the contribution which groundwater makes to improving heat transfer performance of GHEs can be comprehended; this can further promote the development of GSHP technology.

Acknowledgement

The work described in this paper was supported by a GRF grant from The Hong Kong RGC General Research Fund (RGC No: Polyu 152190/14E), and was partially supported by a grant from The Hong Kong RGC General Research Fund (RGC No: Polyu 5176/13E) and by The Hong Kong Polytechnic University Research Institute for Sustainable Urban Development (RISUD).

References

[1] Diao N.R., Fang Z.H., Ground-Coupled Heat Pump Technology. 1st ed. Beijing: Higher Education Press, 2006.

[2] Carslaw H.S., Jeager J. C., Conduction of Heat in Solids, 2th ed. Oxford Press, Oxford, 1959.

[3] Li M. , Lai A.C.K., Analytical model for short-time responses of ground heat exchangers with U-shaped tubes: Model development and validation. Applied Energy. 104(2013) 510-516.

[4] Wu J.L., Zou Z.X., Gong J., Heat transfer analysis of underground heat exchangers under coupled thermal conduction and groundwater advection , Journal of Liaoning Technical University. 28 (2009) 246-248.

[5] Zanchini E., Lazzari S., Priarone A., Long-term performance of large borehole heat exchanger fields with unbalanced seasonal loads and groundwater flow, Energy. 38 (2012) 66-77.

[6] Go G.H., Lee S.R., Yoon S., Kang H.b., Design of spiral coil PHC energy pile considering effective borehole thermal resistance and groundwater advection effects, Applied Energy.125 (2014) 165-178.

[7] Fan R., Jiang Y.Q., Yao Y., etc. A study on the performance of a geothermal heat exchanger under coupled heat conduction and groundwater advection, Energy.32 (2007) 2199–2209.

[8] Capozza A., De Carli M., Zarrella A., Investigations on the influence of aquifers on the ground temperature in ground-source heat pump operation, Applied Energy.107 (2013) 350-363.

[9]Wang F.H., Yu B., Yan L., Heat transfer analysis of groundwater seepage for multi pipe heat exchanger of ground source heat pump, CIESC Journal.61(S2) (2010) 62-67.

[10] Allen A., Milenic D., Low-enthalpy geothermal energy resources from groundwater in fluvioglacial gravels of buried valleys, Applied Energy. 74 (2003) 9-19.

[11] Diao N.R., Li Q.Y., Fang Z.H., Heat transfer in ground heat exchangers with groundwater advection, International Journal of Thermal Sciences. 43 (2004) 1203–1211.

[12] Yu M.Z., Peng X.F., etc. Method for Determining Deep Ground Thermal Properties Accounting for Water Advection, Journal of Basic Science and Engineering.15(2) (2007) 196-202.

[13]Yu M.Z, Fang Z.H., A Method for the On-site Testing of Average Thermo-physical Parameters of Underground Rock Soil, Journal of Engineering for Thermal Energy& Power.17(5) (2002) 489-492.

[14] Ling C., Liu G., Jia M., Study of Soil Thermal Properties and Underground Heat Exchanger Performance, Building Energy&Environment. 31(2) (2012) 15-18.

[15] Sivasakthivel T., Murugesan K., Thomas H.R., Optimization of operating parameters of ground source heat pump system for space heating and cooling by Taguchi method and utility concept, Applied Energy.166(2014) 76-85.

[16] Ye Q.X., Shen Y.H., Handbook of Applied Mathematics, 2nd ed, Beijing, Science Press, 2006.

[17] Department of Mathematics, Tongji University. Advanced Mathematics, 6th ed, Beijing, Higher Education Press, 2007.

[18] Molina-Giraldo N., Blum P., Zhu K., Bayer P., Fang Z.H., A moving finite line source model to simulate borehole heat exchangers with groundwater advection, International Journal of Thermal Sciences.50 (2011) 2506-2513.

[19] Xu L.Z., Modern Mathematics Handbook, 1st ed, Wuhan: Huazhong University of Science & Technology Press, 1999.

[20] Zhang W.K., Yang H.X., etc. The research on ring-coil heat transfer models of pile foundationground heat exchangers in the case of groundwater seepage, Energy and Buildings. 71(2014)115-128.
[21] Lin Y., Further Study on Heat Transfer Model and Design of Geothermal Heat Exchangers, Master Thesis, Department of Thermal Engineering, Shandong Jianzhu University, 2010.
[22] Eskilson P. Thermal Analysis of Heat Extraction Boreholes, Doctoral Thesis, University of Lund, Department of Mathematical Physics, Lund, Sweden,1987.
[23] Liu H., Jin H., Xing S.Y., etc. Influence of Groundwater Seepage on GHE Temperature Field, Water Resources and Power.30(12)(2012)117-119.
[24] Choi J.C., Park J., Lee S.R., Numerical evaluation of the effects of groundwater flow on borehole heat exchanger arrays, Renewable Energy. 52(2013) 230-240.
[25] Raymond J., Lamarche L., Simulation of thermal response tests in a layered subsurface, Applied Energy.109(2013) 293-301.
[26] Witte H.J.L., Error analysis of thermal response tests, Applied Energy.109(2013)302-311.
[27] Park H., Lee S.R., Yoon S., Choi J.C., Evaluation of thermal response and performance of PHC energy pile: Field experiments and numerical simulation, Applied Energy. 103(2013)12-24.
[28] Gao T., Yang H., Liu Y.L., Novel Algorithm for Backward Simulation Using FEM, Chinese construction machinery, 17(19) (2006): 1981-1983.